J. Biochem. **124**, 396-403 (1998)

Influence of Mutation of the Amino-Terminal Signal Anchor Sequence of Cytochrome P450 2B4 on the Enzyme Structure and Electron Transfer Processes[1]

Michael Lehnerer,* Johannes Schulze,* Steven J. Pernecky,† David F.V. Lewis,‡ Manfred Eulitz,§ and Peter Hlavica*,[2]

* *Walther-Straub-Institut für Pharmakologie und Toxikologie der LMU, Nussbaumstrasse 26, D-80336 München, Germany;* † *Department of Chemistry, Eastern Michigan University, Ypsilanti, Michigan 48197, USA;* ‡ *Molecular Toxicology Group, School of Biological Sciences, University of Surrey, Guildford GU2 5XH, UK; and* § *Institut für Klinische Molekularbiologie und Tumorgenetik der GSF, Marchioninistrasse 25, D-81377 München, Germany*

Received for publication, March 16, 1998

The role of the NH_2-terminal hydrophobic patch of cytochrome P4502B4 (CYP2B4) in interactions with NADPH-cytochrome P450 reductase (P450R) and cytochrome b_5 (b_5) was assessed using a variant lacking the signal anchor sequence (Δ2-27). CD, second-derivative, and fluorescence emission spectra indicated that the structure of the deletion mutant slightly differed from that of the native CYP2B4. Fitting of the initial-velocity patterns for P450R- and b_5-directed electron transfer to the ferric CYP2B4 forms to Michaelis-Menten kinetics revealed an approximately 2.3-fold decrease in the affinity of the two electron donors for the engineered enzyme, while the reductive efficiency remained unaffected. Circumstantial analysis suggested that impaired association of the redox proteins with P4502B4(Δ2-27) accounted for this phenomenon. Interestingly, spectral docking of P450R to the truncated pigment was not hampered, while the binding of b_5 was blocked. The rates of substrate-triggered aerobic NADPH consumption in systems containing CYP2B4(Δ2-27) and P450R were 16 to 56% those obtained with the unchanged hemoprotein. Decelerated cofactor oxidation did not arise on defective substrate binding or perturbed utilization of the substrate-bound oxy complex. Experiments with b_5 as the ultimate electron donor hinted at some damage to second-electron transfer to the truncated enzyme. The results are consistent with the proposal that the NH_2-terminal hydrophobic region of CYP2B4 might be of importance in preservation of the catalytic competence of the enzyme.

Key words: cytochrome P450 2B4, electron transfer processes, NH_2-terminus, site-directed mutagenesis.

Cytochrome P450 (P450 or CYP) enzymes, a superfamily of hemoproteins, are major catalysts involved in the oxidation of a diversity of endogenous and exogenous compounds (*1*). Although NADPH-P450 oxidoreductase (P450R) and phospholipid have long been recognized to constitute regular components of the P450-dependent electron-transport chain (*2*), the role of cytochrome b_5 (b_5) as an intermediate carrier appears to be more complex, as it can either enhance or inhibit P450-catalyzed activities in an isoform-specific manner (*3*). Interest has been focused on the molecular basis of functional complex formation between P450 cytochromes and their redox partners. Available evidence arising from studies with chemically modified cytochromes and heterologously expressed mutants hints at electrostatic attraction *via* a charge-pairing mechanism, where carboxylate groups on the P450R and b_5 polypeptides (*4, 5*) as well as positively charged residues on the surface of the diverse P450 subforms (*6-8*) govern donor/acceptor recognition. In addition, repulsive forces, providing a certain looseness required for optimal spacial orientation of the electron transfer interfaces, might be operative (*9*).

The hydrophobic NH_2-terminal region of microsomal P450 isozymes contains a noncleavable sequence generally believed to act as the anchor to the membrane (*10*). Apart from this function, the segment might be of importance in maintaining the catalytic competence. Thus, selective deletion of the membrane-insertion signal peptide in certain P450 species such as CYP1A2, CYP2B4, and CYP7 results in substantially diminished activity toward a number of substrates (*11-13*). One explanation for this observation might be that the NH_2-terminal domain influences the catalytic turnover through interaction with P450R, as demonstrated by the requirement of CYP1A2 and CYP52A3 for a higher reductase concentration to sustain the same level of activity following NH_2-terminal truncation (*11, 14*).

[1] This work was supported by Grant Hl 1/15-1 from the Deutsche Forschungsgemeinschaft.

[2] To whom correspondence should be addressed. Phone: +49-51452-219, Fax: +49-51452-224.

Abbreviations: P450 or CYP, cytochrome P450 [EC 1.14.14.1]; b_5, cytochrome b_5; P450R, NADPH-cytochrome P450 reductase [EC 1.6.2.4]; b5R, NADH-cytochrome b_5 reductase [EC 1.6.2.2]; SDS-PAGE, sodium dodecylsulfate-polyacrylamide gel electrophoresis.

To better answer some questions on the particular role of the hydrophobic NH_2-terminal signal peptide in P450 enzymes in their functional coupling to natural electron donors, we chose to heterologously express a truncated derivative of CYP2B4 lacking amino acid residues 2-27 in *Escherichia coli*. The impact of modification of the hemoprotein on its structure and productive interactions with P450R and b_5 is described in detail.

MATERIALS AND METHODS

Materials—NAD(P)H, glucose oxidase [EC 1.1.3.4], and catalase [EC 1.11.1.6] were obtained from Boehringer (Mannheim, Germany). Dilauroyl L-α-phosphatidylcholine, ethoxycoumarin, benzphetamine, hexobarbital, cumene hydroperoxide, and guanidinium hydrochloride were purchased from Sigma (Deisenhofen, Germany). All other reagents were of the highest purity commercially available.

Protein Expression and Purification—CYP2B4(Δ2-27) was expressed fused to glutathione *S*-transferase in *E. coli* host strain JM109 (Stratagene, Heidelberg, Germany), liberated from the transferase moiety by thrombin treatment, and purified to a specific content of 10.4 nmol P450/mg protein exactly as described previously (*12*). The concentration of the recombinant pigment was determined as indicated by Omura and Sato (*15*) using an absorption coefficient of 91 $mM^{-1} \cdot cm^{-1}$. Final preparations were submitted to analysis by SDS-PAGE on slab gels containing 7.5% acrylamide (*16*), followed by Western blotting (*17*) using a polyclonal antibody against CYP2B.

Full-length CYP2B4 and b_5 were purified to apparent electrophoretic homogeneity by established procedures (*18, 19*) from hepatic microsomes of male New Zealand White rabbits pretreated with phenobarbital (50 mg/kg) for 7 consecutive days; the specific hemoprotein content of the final preparations averaged 17.4 nmol/mg protein and 47 nmol/mg protein, respectively.

P450R and NADH-b_5 oxidoreductase (b5R), isolated from rabbit liver microsomal fractions as reported elsewhere (*18, 20*), exhibited specific activities of 40 μmol of cytochrome *c* reduced/min per mg protein and 970 μmol $K_3Fe(CN)_6$ reduced/min per mg protein, respectively. The two flavoproteins were quantified on the basis of their absorbance at 456 nm using absorption coefficients of 10 and 21.4 $mM^{-1} \cdot cm^{-1}$ (*21, 22*), respectively.

Spectral Measurements—Spectral analysis was carried out at room temperature with a Shimadzu UV-265FW spectrophotometer. The standard conditions for measuring second-derivative spectra were as follows: scan speed, 60 nm/min; slit width, 1 nm; $\Delta\lambda$, 2 nm. The assay media consisted of P450 protein (3.6 μg/ml) in 50 mM sodium phosphate (pH 7.0); the pH was adjusted to 6.5 with buffer supplemented with 6 M guanidinium hydrochloride. The fraction of tyrosine residues exposed to solvent (α) was assessed using the equation (*23*)

$$\alpha = (r_n - r_a)/(r_u - r_a)$$

where r_n and r_u are the numerical values of the ratio (a/b) of the trough-to-peak second-derivative spectral differences with the wavelength pairs 282.5/287 nm and 290.8/296 nm, respectively, for the native pigment and protein unfolded in the presence of a chaotropic agent; and r_a is the a/b value of an assay mixture containing the same molar ratio of aromatic amino acids dissolved in a medium possessing the characteristics of the interior of the protein matrix. In this case, r_a was computed using coefficients relative to ethylene glycol, as indicated elsewhere (*23*).

Fluorescence emission spectra were obtained with the P450 protein (32 pg/ml) in 10 mM sodium phosphate (pH 7.4) with a Shimadzu RF-1502 spectrofluorimeter; the excitation wavelength was 280 nm. Protein concentrations were determined by the method of Lowry *et al.* (*24*).

CD spectra in the far ultraviolet and visible regions were recorded at room temperature with a Jasco J-500A spectropolarimeter; the optical pathlengths were 0.02 and 1.0 cm, respectively. Measurements were conducted in 50 mM sodium phosphate (pH 7.4) containing 2.6 to 5 μM P450. Mean residue ellipticities were calculated using a value of 110 for the mean residue weight. The helical content (f_H) was roughly estimated with the empirical equation (*25*)

$$f_H = -([\theta]_{208} + 4{,}000)/29{,}000$$

where $[\theta]_{208}$ represents the ellipticity at 208 nm.

Titration of P450 with substrates (hexobarbital, benzphetamine, and ethoxycoumarin) was carried out in 150 mM sodium phosphate (pH 7.4) containing 1 μM hemoprotein; the substrate concentrations ranged from 0.1 to 2.0 mM. Adduct formation was quantified at 25°C by monitoring the absorbance change at 383 nm relative to that at 419 nm.

Binding of P450R and b_5 to P450 was studied using matched tandem cuvettes. The assay mixtures consisted of 4 μM P450, 40 μM dilauroyl phosphatidylcholine, and 0.2 μM P450R (or 3 μM b_5) in 150 mM sodium phosphate (pH 7.4). Formation of the high-spin complexes was followed at 25°C by scanning difference spectra in the region from 360 to 430 nm; the optical pathlength was 1.0 cm.

Enzyme Assays—NAD(P)H-supported reduction of ferric P450 was measured at 25°C in reaction mixtures comprising 2 μM P450, varying amounts of P450R (or b_5 plus 0.5 μM b5R), 40 μM dilauroyl phosphatidylcholine (sonicated until clarification was observed), 1 mM hexobarbital, 100 mM glucose, glucose oxidase (400 μg/ml), and catalase (80 μg/ml) in 150 mM sodium phosphate (pH 7.4). The system was preincubated at room temperature for 15 min to allow efficient association of the redox proteins in the micellar system. Subsequently, the samples were gassed for 5 min with CO; this time period was sufficient to establish anaerobiosis (*6*). Reactions were initiated by the rapid addition of NAD(P)H to yield final concentrations of 0.1 to 0.33 mM using a set of plunger cuvettes. When the chemical reduction of P450 was examined, the components of the natural electron transfer system were omitted, and the hemoprotein was reduced by the addition of $Na_2S_2O_4$ to give a final concentration of 10 mM. Absorbance changes at 450 nm relative to that at 500 nm were recorded with an Aminco DW-2 spectrophotometer operated in the dual-wavelength mode.

In some studies, the rates of reduction were measured in systems in which P450 and P450R or b_5 were not in the preformed complexes described above. In this case, 4 μM P450 and 0.2 μM P450R (or 1 μM b_5 plus 1 μM b5R) were separately combined in two syringes with 40 μM phospholipid in the presence of 1 mM hexobarbital, 1 mM NAD(P)H, and a deoxygenating system, followed by incubation at 25°C for 15 min. After gentle bubbling of the mixtures with

CO, the syringes were transferred to an Aminco Dasar/DW-2 spectrophotometer equipped with an Aminco-Morrow stopped-flow apparatus with a dead time of 4 ms. The extent of reduction was determined by monitoring the formation of the carbonyl adduct of ferrous P450 at 450 nm upon rapid mixing of the contents of the syringes.

NAD(P)H oxidase activity was assayed at 25°C by recording the decrease in absorbance at 340 nm in media composed of 2 μM P450, 0.5 μM P450R (or 6 μM b_5 plus 0.5 μM b5R), 40 μM dilauroyl phosphatidylcholine, 50 μM NAD(P)H, and 1 mM substrate (hexobarbital, benzphetamine, or ethoxycoumarin) in 150 mM sodium phosphate (pH 7.4); controls in the absence of substrate were run simultaneously.

The kinetics of consumption of the substrate-bound oxy-complex of P450 were assessed by scanning the decrease in absorbance at 440 nm after rapid mixing in the stopped-flow apparatus of two solutions, one of which was prepared to yield 4 μM P450, 80 μM dilauroyl phosphatidylcholine, and 2 mM hexobarbital in 150 mM sodium phosphate (pH 7.4); and the other solution comprised 10 mM cumene hydroperoxide in the same buffer.

Molecular Modeling—Structure investigations on P450 were carried out according to a recent three-dimensional model of CYP2B4 based on multiple protein sequence homology alignment with the CYP102 template. The model was constructed and refined using the Sybyl Biopolymer and Tripos force field protein analysis programs as described previously (*26*).

RESULTS AND DISCUSSION

Spectral Characterization of CYP2B4(Δ2-27)—CYP-2B4 lacking amino acid residues 2-27 (Table I) was expressed in *E. coli* fused to glutathione *S*-transferase and purified following cleavage of the protein with thrombin. The truncated pigment did not undergo degradation during the expression and purification processes, as evidenced by immunoblot analysis (data not shown). The A_{418}/A_{390} ratio in the electronic spectrum of oxidized CYP2B4 (Δ2-27) was of 2.1. The truncated hemoprotein generated a normal CO-reduced difference spectrum, the Soret band being centered around 451 nm. These spectral characteristics were comparable with those reported for low-spin CYP2B4 purified from phenobarbital-treated rabbit liver microsomal fractions (*27*). Thus, at first glance, the structure of the truncated enzyme did not appear to grossly differ from that of the native pigment. However, CD-spectral analysis in the far ultraviolet region revealed attenuation of the signal amplitude for the mutant enzyme as compared to that for CYP2B4 (Fig. 1A), all spectra being corrected for the apohemoprotein concentration on the basis of the A_{418}/A_{280} ratios of the individual preparations (*28*). Taking the mean residue ellipticities at 208 nm to be −23,400 (±600 SE; $n=3$) and −20,100 (±600 SE; $n=3$) deg·cm²·dmol⁻¹ for the native and truncated hemoprotein, respectively, the α-helix content (f_H) could be determined (*25*) to decrease significantly from 65 to 55% ($p<0.02$) upon removal of amino acids 2-27. In contrast, the spectra obtained in the Soret region of the two enzyme forms were virtually superimposable (Fig. 1B), suggesting that the structural alteration seen did not affect the geometry of the immediate heme environment.

The question arose as to whether the decrease in the α-helix content observed with the truncated variant (Fig. 1A) simply resulted from loss of the helical anchor segment of CYP2B4, or reflected some additional conformational change in the truncated hemoprotein. The answer to this was provided by studies designed to examine more closely the impact of truncation of the hydrophobic NH_2-terminus of CYP2B4 on the local environment of aromatic amino acids such as tyrosine and tryptophan, the latter not occurring within the critical region spanning residues 2-27. To this end, second-derivative spectroscopy was performed, offering a means of high-resolution of spectral bands ascribable to tyrosine (*23*). As shown in Fig. 2, there was a pronounced difference in the ratios (a/b) of the trough-to-peak differences with two definite wavelength pairs between CYP2B4 and its truncated variant. Unfolding of the proteins in the presence of 6 M guanidinium hydrochloride mainly affected the signal amplitude at the wavelengths of 282.5-287 nm, which is indicative of a polarity change in the tyrosine environment. From the spectral data obtained in the absence and presence of the chaotropic agent, the fraction (α) of tyrosines exposed to the solvent of the native and truncated hemoprotein could be calculated to be 0.81 and 0.73, applying the procedure of Ragone *et al.* (*23*). Assuming a total of 12 tyrosines was available per polypep-

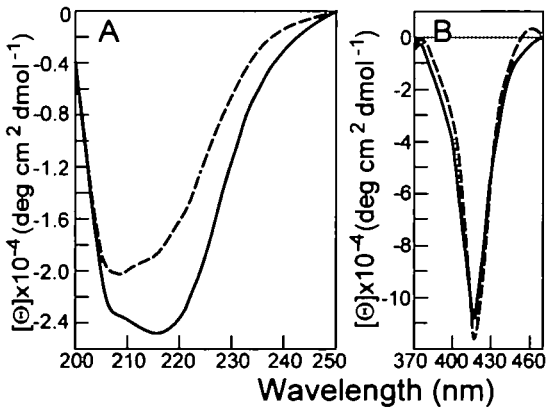

Fig. 1. **CD spectra of native and truncated CYP2B4.** CD spectra in the far ultraviolet (A) and visible (B) regions were recorded for solutions containing 2.6 to 5 μM native (—) or truncated (- - -) CYP 2B4 protein in 50 mM sodium phosphate (pH 7.4).

TABLE I. **Amino-terminal sequences of full-length and truncated CYP2B4.** CYP2B4(Δ2-27), a truncated variant of CYP2B4 lacking residues 2-27, was expressed fused to glutathione *S*-transferase. Alanine was introduced to position 2 of the truncated polypeptide to create a thrombin binding site required for efficient cleavage of the fusion protein (*12*).

P450 variant	NH_2-terminal sequence
	10 20 30 40
CYP2B4	MEFSLLLLLAFLAGLLLLLFRGHPKAHGRLPPGPSPLPVL
CYP2B4(Δ2-27)	MA----------GRLPPGPSPLPVL

tide (*29*), the numbers of exposed residues in the two P450 forms thus were determined to be 9.6 and 8.6, respectively, per mole of enzyme, suggesting that one tyrosine residue originally accessible to the solvent became buried upon NH_2-terminal modification of CYP2B4.

Typical fluorescence emission profiles of CYP2B4 consistently exhibited a broad band centered around 335 nm (Fig. 3), arising from excitation of the single tryptophan residue located at position 121 (*30*). Removal of the NH_2-terminal region resulted in an increase in fluorescence efficiency associated with a shift of the emission peak to 305-307 nm (Fig. 3). These phenomena could be understood on the basis of the preferential interaction of the ^1L_a transition state of the indole side chain of tryptophan with polar solvents owing to the larger change in its permanent dipole moment, it thus being sensitive to variations in the dielectric constant of the local environment (*31*). Indeed, the strongly hydrophobic surroundings of the single tryptophan in bacterial azurin have been advocated to be the cause of the 308-nm emission maximum of this residue (*32*). As the interior of proteins is believed to be characterized by very low dielectric constants (*33*), the most plausible explanation for the strong blue shift of the emission band observed with CYP2B4(Δ2-27) was that Trp-121, assumed to be partly accessible to the solvent in native CYP2B4 (*30*), became buried upon deletion of amino acids 2-27. Alternatively, an orientation constraint due to a structural change in the immediate vicinity of the fluorophore might have caused energy loss during the lifetime of the excited state. Tyrosine-tryptophan energy transfer did not seem to be operative, since the use of light of the wavelength of 293 nm, which allows tryptophan fluorescence to be excited independently of that of tyrosine (*31*), did not affect the position of the emission maximum of the truncated enzyme. It should be pointed out that highly conserved Trp-121 has been shown to reside within the boundary of a CYP2B4 domain regarded as representative of a so-called Rossman motif, which is known to accomodate amino acid residues involved in contacts with electron donors (*34*). Figure 4 presents a three-dimensional view of the spacial relationship between the critical tryptophan and the NH_2-terminal region of CYP2B4.

In conclusion, truncation of CYP2B4 was found to influence the conformational integrity of the polypeptide at site(s) remote from the NH_2-terminus. Such a long-range effect does not seem to be unique. Thus, residues 22-28 in CYP2C2 have been recognized to affect efficient assembly of the protein into a functional form (*35*).

Reduction Kinetics of Ferric CYP2B4(Δ2-27) under

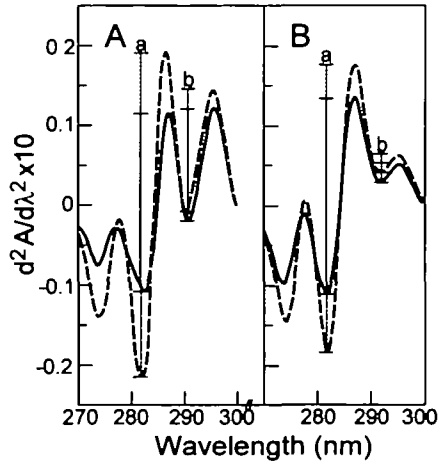

Fig. 2. **Second-derivative spectra of native and truncated CYP2B4.** (A) Spectra were obtained with the native (—) or truncated (- - -) CYP2B4 protein (3.6 μg/ml) dissolved in 50 mM sodium phosphate (pH 7.0). (B) The conditions were as in (A), except that the pigments were treated with 6 M guanidinium hydrochloride at pH 6.5; a and b denote trough-to-peak second-derivative absorbance differences.

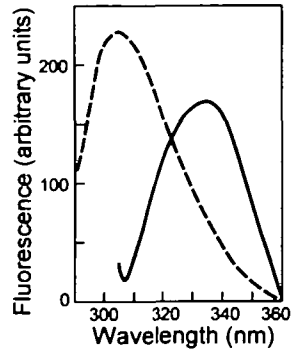

Fig. 3. **Fluorescence emission spectra of native and truncated CYP2B4.** Fluorescence emission spectra were recorded for solutions containing the native (—) or truncated (- - -) CYP2B4 protein (32 pg/ml) in 10 mM sodium phosphate (pH 7.4); the excitation wavelength was 280 nm.

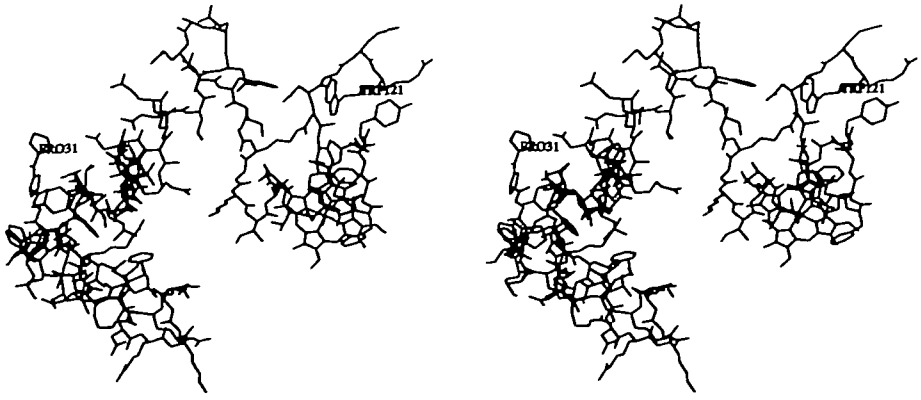

Fig. 4. **Stereodiagram of the topology of Trp-121 in the CYP2B4 model.** The view displays the putative Rossman motif, comprising three α-helices (A, B, and B′) and three strands of a β_1-sheet (all in blue), with Pro-31 (in black) residing in the NH_2-terminal region of CYP2B4 (see also Table I) and Trp-121 (in green) being present close to the start of the putative C helix. Also shown is the position of the heme unit (in magenta) relative to the conserved tryptophan residue.

Anaerobic Conditions—The slight structural rearrangement on the surface of CYP2B4(⊿2-27), as suggested by the spectral data, prompted us to look for a potential impact of this change on functional parameters, such as electron transfer to the ferric pigment. These studies were of special interest, since previous investigations on the role of the first hydrophobic segment of CYP2B4 in electron transfer events yielded contradictory results (*12, 28*).

Measurements were conducted under strictly anaerobic conditions to avoid autoxidation of the terminal acceptor, so that the observed velocities of accumulation of the ferrous pigment primarily reflected the rates of electron transfer. Using $Na_2S_2O_4$ as the chemical reductant, the basic acceptor properties of the truncated enzyme were shown to be equivalent to those of CYP2B4, as evidenced by a uniform rate constant of 1.73 min^{-1} for electron transfer to the two pigments. Alternatively, NADPH-dependent, hexobarbital-stimulated electron flow was assessed in reconstituted micellar systems containing P450R and P450 at molar ratios varying from 1:5 to 1:80. Double-reciprocal plots of reduction activity *versus* P450R concentration disclosed a 2.3-fold increase in the apparent K_m value for the truncated variant as compared with that of CYP2B4, while the efficiency of electron transfer (V_{max} value) remained unchanged (Fig. 5A). That the observed decrease in affinity for P450R resulted from aberrant partitioning of the truncated CYP2B4 form between the lipid and aqueous phases of the assay medium to diminish the statistical probability of the redox partners to encounter one another seemed unlikely: the extent of P450R-induced type I spectral complex formation, as brought about with CYP2B4(⊿2-27) at a molar ratio of reductase to hemoprotein of 1:20, permitting the NADPH-driven reduction of the truncated enzyme to proceed at a rate about 50% that of the full-length form (*cf.* Fig. 5A), was not appropriately diminished, but rather slightly increased (Fig. 6A). This indicated that removal of the NH_2-terminal hydrophobic patch of CYP2B4 did not hamper the access or binding of the truncated pigment to P450R attached to micelles of phospholipid (*22*). Similarly, the increase in the K_m value for P450R was not due to differences in the aggregation states of the two P450 forms, since CYP2B4 and its truncated derivative uniformly exist as 6- to 8-mers in the absence of an added detergent (*12*). The data thus suggested the requirement of CYP2B4 for a significantly higher P450R concentration to maintain the same rate of electron transfer upon removal of the NH_2-terminus.

Like P450R, b_5 exhibited a significant decrease in reactivity toward CYP2B4(⊿2-27) with undisturbed reductive capacity, when NADH-sustained electron flow was examined in the presence of barbiturate in reconstituted micellar systems containing b_5/b5R and P450 bound to phospholipid (Fig. 5B).

When substrate-bound P450 was rapidly mixed with NAD(P)H-reduced P450R or b_5 in the presence of phospholipid under anaerobic conditions, so that association of the redox proteins constituted the rate-limiting step in electron transfer, the rates of reduction of CYP2B4(⊿2-27) by b_5 or P450R were found to be 12 and 47%, respectively,

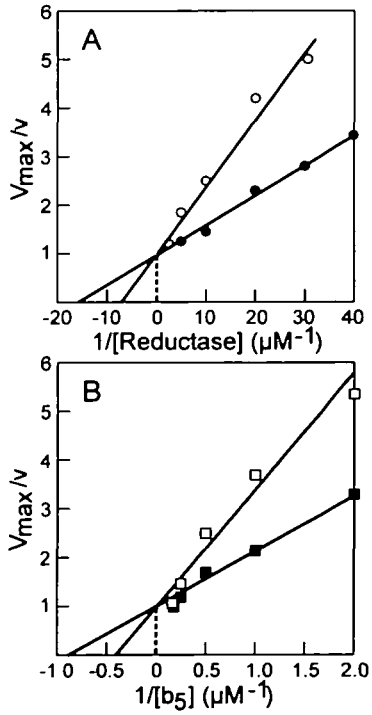

Fig. 5. **Influence of truncation of CYP2B4 on the initial-velocity pattern of NAD(P)H-sustained enzyme reduction.** The initial rates (v) of hexobarbital-stimulated, NAD(P)H-driven electron transfer to the native (●, ■) or truncated (○, □) CYP2B4 in systems containing phospholipid and either P450R (A) or b_5/b5R (B) as the electron donors were fitted to Michealis-Menten kinetics to yield V_{max} values for the reduction processes, *i.e.* 130 and 70 pmol P450 reduced/min, respectively; for details see under "MATERIALS AND METHODS." The lines were obtained by non-linear regression analysis using the Corel QuattroPro 7.0 software. The points are the means of three experiments.

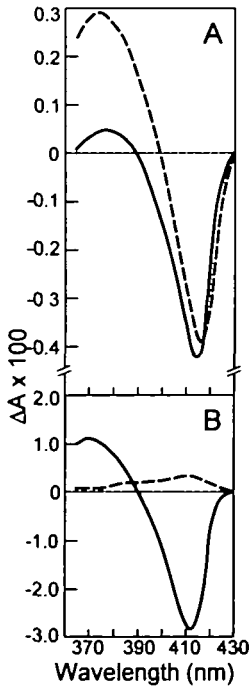

Fig. 6. **Spectral binding of redox proteins to native and truncated CYP2B4.** Difference spectra were obtained by reacting 0.2 μM P450R (A) or 3 μM b_5 (B) with 4 μM native (——) or truncated (- - -) CYP2B4 reconstituted into phospholipid.

those of the corresponding CYP2B4-catalyzed reactions (Fig. 7), suggesting that impaired association rather than decreased complex stability played a preponderant role in the change in the affinity for each other of the redox components (Fig. 5).

As regards the process of association, CYP2B4 contains distinct contact regions controlling either non-productive spectral binding of the redox partners or functional alignment of the electron transfer interfaces (*6, 36*). On comparison of the spectral and kinetic data presented in Figs. 6A and 7A, as measured with media containing P450R and P450 in the same molar ratio, truncation of CYP2B4 did not appear to compromise the association of P450R *via* disturbed binding of the flavo- to the hemoprotein. Hence, some damage to the mechanism(s) governing electron acceptance was assumed to be responsible for the observed phenomenon. In view of the relatively large distance between the α-amino group and the heme plane of CYP2B4, a direct effect of modification of the hydrophobic tail portion on electron tunneling seemed unlikely (*28*). Rather, the data obtained from the second-derivative, fluorescence and CD spectra (Figs. 1-3) suggested that truncation of CYP2B4 perturbed folding of the pigment into a structure competent as to optimal productive coupling of P450R.

In the case of b_5, the hampered association of the intermediate carrier with CYP2B4(Δ2-27) (Fig. 7B) might have primarily reflected defective binding of the electron donor (Fig. 6B). Recent studies with native or truncated CYP2B4 immobilized on the matrix of an optical biosensor in the absence of phospholipid gave similar results (*37*), suggesting that impaired access of the truncated enzyme to lipid-bound b_5 did not account for the blockage of complexing shown in Fig. 6B. Most strikingly, the observed change, by a factor of 2.3, in the apparent K_m value for b_5 following truncation of CYP2B4 (Fig. 5B) was smaller than would have been anticipated from the severe perturbation of interaction of b_5 with the truncated pigment (*cf.* Figs. 6B and 7B). This discrepancy could be reconciled by assuming that the deleted NH_2-terminal anchor sequence of CYP2B4 was not essential for functional coupling of the intermediate carrier, but exerted limited control over this process, possibly by affecting the proper spacial orientation of b_5 to foster electron transfer events. Clearly, our data do not exclude the possibility that the observed overall affinity of b_5 for the truncated CYP2B4 partly resulted from some additional indirect effect on the protein conformation (Figs. 1-3) following removal of amino acids 2-27.

Catalytic Features of CYP2B4(Δ2-27) under Aerobic Conditions—To further characterize the effect of truncation of CYP2B4 on its catalytic properties, NADPH oxidation was measured in aerobic media containing P450/P450R, phospholipid and substrate. In such systems, CYP2B4-dependent NADPH utilization is known to be tightly coupled to substrate oxidation (*38*). Stimulated NADPH consumption was corrected for low NADPH oxidase activity in the absence of added substrate to reflect events associated with overall metabolic transformation of the compounds studied. In order to assess the turnover with a physiologically relevant protein stoichiometry, assays were carried out with a P450R-to-P450 molar ratio far below that routinely used (*38*).

Surprisingly, the initial velocities of NADPH oxidation, as measured with CYP2B4(Δ2-27) in the presence of ethoxycoumarin, hexobarbital or benzphetamine, were 16 to 56% those obtained with CYP2B4 (Table II), indicating that truncation of the native species resulted in substantial impairment of substrate turnover. This effect was not due to hampered transfer of the first electron, since assays were carried out with a molar ratio of P450R to P450 of 1:4, which is sufficient to largely compensate for the diminished affinity of the flavoprotein for the truncated CYP2B4 species (*cf.* Fig. 5A). Uncoupling of the system or poor substrate binding by the truncated enzyme also could be dismissed as accounting for the impaired cofactor oxida-

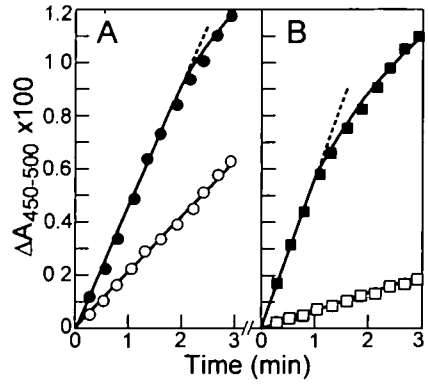

Fig. 7. **Time course of association of native and truncated CYP2B4 with redox partners.** Native CYP2B4 (●, ■) and its truncated derivative (○, □) were reconstituted into sonicated phospholipid and placed in the first syringe of the stopped-flow spectrophotometer together with NAD(P)H and a deoxygenating system. The second syringe contained either P450R (A) or b_5/b5R (B) in the lipid matrix supplemented with a reductant and an O_2-scavenging system as described under "MATERIALS AND METHODS." Both syringes contained hexobarbital prior to mixing. The data points represent the means of three experiments.

TABLE II. **Substrate-triggered NAD(P)H utilization by and substrate binding to native and truncated CYP2B4.** The basic assay medium for measuring NAD(P)H oxidase activity consisted of P450, P450R (or b_5 plus b5R), and dilauroyl phosphatidylcholine; cofactor consumption in the absence and presence of a substrate was followed at 340 nm. Substrate binding was assessed by optical difference spectroscopy in the Soret region (383-419 nm) of P450. The figures in parentheses indicate percentages of values observed with the full-length enzyme. The data are the means ± SE of three experiments.

Substrate added	NAD(P)H oxidation[a] (pmol/min per nmol P450)				Substrate binding ΔA_{max} ($mM^{-1}\cdot cm^{-1}$)	
	NADPH-dependent pathway		NADH-dependent pathway			
	CYP2B4	CYP2B4 (Δ2-27)	CYP2B4	CYP2B4 (Δ2-27)	CYP2B4	CYP2B4(Δ2-27)
Hexobarbital	190± 10	80± 3 (42%)	190±10	180±40 (95%)	4.6±0.3	3.6±0.4 (78%)
Benzphetamine	250± 80	140±40 (56%)	220±10	190±40 (86%)	4.7±0.1	4.6±0.1 (98%)
Ethoxycoumarin	1,200±150	190±70 (16%)	1,010±30	1,210±50 (119%)	5.7±0.2	4.8±0.8 (84%)

[a]Activities were corrected for NAD(P)H consumption in the absence of an added substrate.

tion: previous work demonstrated that the substrate-specific proportion of NADPH utilized/H_2O_2 released in incubation mixtures fortified with benzphetamine or other substrates was almost the same irrespective of whether CYP2B4 or the truncated construct was the catalyst (*39*). Moreover, the ability of the truncated hemoprotein to bind ethoxycoumarin, hexobarbital, and benzphetamine, as determined with substrate concentrations that were in excess of those required to saturate the enzyme, was not severely different from that of CYP2B4 (Table II). Similarly, perturbed oxygen utilization by CYP2B4(⊿2-27) did not appear to be responsible for the hampered substrate turnover, as suggested by the almost identical half-lives of 42 and 48 s, respectively, for the consumption of the cumene hydroperoxide-derived, 440-nm absorbing oxy-enzyme-substrate complexes generated with native and truncated ferricytochrome P450 in the presence of hexobarbital as the model substrate (Fig. 8); the initial rate of breakdown of such organic peroxide-dependent spectral intermediates has been conclusively shown to correlate well with the catalytic capacity of the systems tested (*40, 41*).

The remaining possibility was that truncation of the NH_2-terminus of CYP2B4 affected events involved in the transfer of the second electron. This view was compatible with results of experiments in which P450R, bridging electron flow from NADPH to P450, was replaced with the b_5/b5R chain. On adjustment of the molar ratio of b_5 to P450, such as to permit undisturbed transfer of the first electron (*cf.* Fig. 5B), the rates of substrate-triggered, aerobic NADH consumption, as measured with CYP2B4-(⊿2-27) in the presence of ethoxycoumarin, hexobarbital, or benzphetamine, did not significantly differ from those obtained with the full-length enzyme (Table II). This behaviour was different from that of the NADPH-sustained pathway. An explanation for this might be that, under physiological conditions, b_5 is capable of donating the second electron to members of the CYP2B subfamily at a rate about 3-times that of the P450R-directed transfer, and at even higher velocity when the molar ratio of b_5 to P450 is artificially raised (*42*), as was the case in our studies. This might have more than compensated for the defective interaction of the intermediate carrier with oxyferrous CYP2B4(⊿2-27).

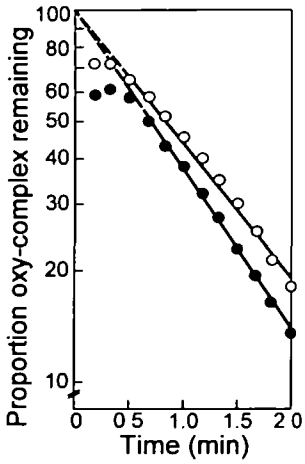

Fig. 8. **Impact of truncation of CYP2B4 on the steady-state level and kinetics of breakdown of the 440-nm-absorbing substrate-bound oxy complex.** The absorbance changes at 440 nm were monitored after rapid mixing of the components to yield final concentrations, in the observation cell of the stopped-flow apparatus, of 2 μM native (●) or truncated (○) CYP2B4 reconstituted into phospholipid, 1 mM hexobarbital, and 5 mM cumene hydroperoxide in 150 mM sodium phosphate (pH 7.4). The data are the means of three experiments.

Collectively, we have presented unequivocal evidence that deletion of amino acids 2-27 in the NH_2-terminal signal anchor sequence of CYP2B4 affects the mechanism(s) governing electron transfer from P450R and b_5. The observed variations in the kinetics of electron flow are likely to be brought about in direct and/or indirect ways. In the latter case, subtle conformational rearrangement(s) at recognition site(s) for the redox partners are thought to influence productive contacts with the electron donors. These findings underline the importance of the hydrophobic tail portion of CYP2B4 for preserving the fully active enzyme. Interestingly, this principle does not appear to be applicable to all types of P450. Thus, the absence of amino acids 3-12 in human CYP3A4 was found to leave the substrate turnover unaffected (*43*). Similarly, removal of residues 3-29 from CYP2E1 neither impairs catalytic efficiency nor the association of P450R and b_5 (*44*). The molecular basis for this discrepant behaviour will be the subject of further studies.

The authors are indepted to Cortina Keiling for the competent technical assistance.

REFERENCES

1. Porter, T.D. and Coon, M.J. (1991) Cytochrome P450. Multiplicity of isoforms, substrates, and catalytic and regulatory mechanisms. *J. Biol. Chem.* **266**, 13469-13472
2. Lu, A.Y.H. and Coon, M.J. (1968) Role of hemoprotein P-450 in fatty acid ω-hydroxylation in a soluble enzyme system from liver microsomes. *J. Biol. Chem.* **243**, 1331-1332
3. Morgan, E.T. and Coon, M.J. (1984) Effects of cytochrome b_5 on cytochrome P-450-catalyzed reactions. Studies with manganese-substituted cytochrome b_5. *Drug Metab. Dispos.* **12**, 358-364
4. Tamburini, P.P. and Schenkman, J.B. (1986) Differences in the mechanism of functional interaction between NADPH-cytochrome P-450 reductase and its redox partners. *Mol. Pharmacol.* **30**, 178-185
5. Tamburini, P.P., White, R.E., and Schenkman, J.B. (1985) Chemical characterization of protein-protein interactions between cytochrome P-450 and cytochrome b_5. *J. Biol. Chem.* **260**, 4007-4015
6. Hlavica, P., Lehnerer, M., and Eulitz, M. (1996) Histidine residues in rabbit liver microsomal cytochrome P-450 2B4 control electron transfer from NADPH-cytochrome P-450 reductase and cytochrome b_5. *Biochem. J.* **318**, 857-862
7. Bernhardt, R., Kraft, R., Otto, A., and Ruckpaul, K. (1988) Electrostatic interactions between cytochrome P-450 LM2 and NADPH-cytochrome P-450 reductase. *Biomed. Biochim. Acta* **47**, 581-592
8. Shen, S. and Strobel, H.W. (1992) The role of cytochrome P450 lysine residues in the interaction between cytochrome P450IA1 and NADPH-cytochrome P450 reductase. *Arch. Biochem. Biophys.* **294**, 83-90
9. Voznesensky, A.I. and Schenkman, J.B. (1992) The cytochrome P450 2B4-NADPH cytochrome P450 reductase electron transfer complex is not formed by charge-pairing. *J. Biol. Chem.* **267**, 14669-14676
10. Haugen, D.A., Armes, L.G., Yasunobu, K.T., and Coon, M.J. (1977) Amino-terminal sequence of phenobarbital-inducible cytochrome P-450 from rabbit liver microsomes: similarity to

hydrophobic amino-terminal segments of preproteins. *Biochem. Biophys. Res. Commun.* **77**, 967-973
11. Dong, M.S., Yamazaki, H., Guo, Z., and Guengerich, F.P. (1996) Recombinant human cytochrome P450 1A2 and an N-terminal-truncated form: construction, purification, aggregation properties, and interactions with flavodoxin, ferredoxin, and NADPH-cytochrome P450 reductase. *Arch. Biochem. Biophys.* **327**, 11-19
12. Pernecky, S.J., Olken, N.M., Bestervelt, L.L., and Coon, M.J. (1995) Subcellular localization, aggregation state, and catalytic activity of microsomal P450 cytochromes modified in the NH_2-terminal region and expressed in *Escherichia coli*. *Arch. Biochem. Biophys.* **318**, 446-456
13. Li, Y.C. and Chiang, J.Y. (1991) The expression of a catalytically active cholesterol 7α-hydroxylase cytochrome P450 in *Escherichia coli*. *J. Biol. Chem.* **266**, 19186-19191
14. Scheller, U., Kraft, R., Schröder, K.L., and Schunck, W.H. (1994) Generation of the soluble and functional cytosolic domain of microsomal cytochrome P450 52A3. *J. Biol. Chem.* **269**, 12779-12783
15. Omura, T. and Sato, R. (1964) The carbon monoxide-binding pigment of liver microsomes. II. Solubilization, purification, and properties. *J. Biol. Chem.* **239**, 2379-2385
16. Laemmli, U.K. (1970) Cleavage of structural proteins during the assembly of the head of bacteriophage T4. *Nature* **227**, 680-685
17. Towbin, H., Staehelin, T., and Gordon, J. (1979) Electrophoretic transfer of proteins from polyacrylamide gels to nitrocellulose sheets: procedure and some applications. *Proc. Natl. Acad. Sci. USA* **76**, 4350-4354
18. Hlavica, P. and Hülsmann, S. (1979) Studies of the mechanism of hepatic microsomal *N*-oxide formation. *N*-oxidation of *N,N*-dimethylaniline by a reconstituted rabbit liver microsomal cytochrome P-448 enzyme system. *Biochem. J.* **182**, 109-116
19. Strittmatter, P., Fleming, P., Connors, M., and Corcoran, D. (1978) Purification of cytochrome b_5. *Methods Enzymol.* **52**, 97-101
20. Mihara, K. and Sato, R. (1978) Detergent-solubilized NADH-cytochrome b_5 reductase. *Methods Enzymol.* **52**, 102-108
21. Tamburini, P.P. and Schenkman, J.B. (1987) Purification to homogeneity and enzymological characterization of a functional covalent complex composed of cytochromes P-450 isozyme 2 and b_5 from rabbit liver. *Proc. Natl. Acad. Sci. USA* **84**, 11-15
22. French, J.S., Guengerich, F.P., and Coon, M.J. (1980) Interactions of cytochrome P-450, NADPH-cytochrome P-450 reductase, phospholipid, and substrate in the reconstituted liver microsomal enzyme system. *J. Biol. Chem.* **255**, 4112-4119
23. Ragone, R., Colonna, G., Balestrieri, C., Servillo, L., and Irace, G. (1984) Determination of tyrosine exposure in proteins by second-derivative spectroscopy. *Biochemistry* **23**, 1871-1875
24. Lowry, O.H., Rosebrough, N.J., Farr, A.L., and Randall, R.J. (1951) Protein measurement with the Folin phenol reagent. *J. Biol. Chem.* **193**, 265-275
25. Greenfield, N. and Fasman, G.D. (1969) Computed circular dichroism spectra for the evaluation of protein conformation. *Biochemistry* **8**, 4108-4116
26. Lewis, D.F.V. and Lake, B.G. (1997) Molecular modelling of mammalian CYP2B isoforms and their interaction with substrates, inhibitors and redox partners. *Xenobiotica* **27**, 443-478
27. Haugen, D.A. and Coon, M.J. (1976) Properties of electrophoretically homogenous phenobarbital-inducible and β-naphthoflavone-inducible forms of liver microsomal cytochrome P-450. *J. Biol. Chem.* **251**, 7929-7939
28. Schwarze, W., Bernhardt, R., Jänig, G.R., and Ruckpaul, K. (1983) Fluorescent energy transfer measurements on fluorescein isothiocyanate modified cytochrome P-450 LM2. *Biochem. Biophys. Res. Commun.* **113**, 353-360
29. Tarr, G.E., Black, S.D., Fujita, V.S., and Coon, M.J. (1983) Complete amino acid sequence and predicted membrane topology of phenobarbital-induced cytochrome P-450 (isozyme 2) from rabbit liver microsomes. *Proc. Natl. Acad. Sci. USA* **80**, 6552-6556
30. Inouye, K. and Coon, M.J. (1985) Properties of the tryptophan residues in rabbit liver microsomal cytochrome P-450 isozyme 2 as determined by fluorescence. *Biochem. Biophys. Res. Commun.* **128**, 676-682
31. Ross, J.B.A., Szabo, A.G., and Hogue, C.W.V. (1997) Enhancement of protein spectra with tryptophan analogs: fluorescence spectroscopy of protein-protein and protein-nucleic acid interactions. *Methods Enzymol.* **278**, 151-190
32. Finazzi-Agro, A., Rotilio, G., Avigliano, L., Guerrieri, P., Boffi, V., and Mondovi, B. (1970) Environment of copper in *Pseudomonas fluorescens* azurin: fluorimetric approach. *Biochemistry* **9**, 2009-2014
33. Schulz, G.E. and Schirmer, R.H. (1978) *Principles of Protein Structure*, p. 30, Springer-Verlag, Berlin
34. Tretiakov, V.E., Degtyarenko, K.N., Uvarov, V.Y., and Archakov, A.I. (1989) Secondary structure and membrane topology of cytochrome P450s. *Arch. Biochem. Biophys.* **275**, 429-439
35. Chen, C.D., Doray, B., and Kemper, B. (1997) Efficient assembly of functional cytochrome P450 2C2 requires a spacer sequence between the N-terminal signal anchor and catalytic domains. *J. Biol. Chem.* **272**, 22891-22897
36. Davydov, D.R., Knyushko, T.V., Kanaeva, I.P., Koen, Y.M., Samenkova, N.F., Archakov, A.I., and Hui Bon Hoa, G. (1996) Interactions of cytochrome P450 2B4 with NADPH-cytochrome P450 reductase studied by fluorescent probe. *Biochimie* **78**, 734-743
37. Ivanov, Y.D., Kanaeva, I.P., Eldarov, M.A., Skryabin, K.G., Lehnerer, M., Schulze, J., Hlavica, P., and Archakov, A.I. (1997) An optical biosensor study of the interaction parameters and role of hydrophobic tails of cytochrome P450 2B4, b_5 and NADPH-flavoprotein in complex formation. *Biochem. Mol. Biol. Int.* **42**, 731-737
38. Nordblom, G.D. and Coon, M.J. (1977) Hydrogen peroxide formation and stoichiometry of hydroxylation reactions catalyzed by highly purified liver microsomal cytochrome P-450. *Arch. Biochem. Biophys.* **180**, 343-347
39. Vaz, A.D.N., Pernecky, S.J., Raner, G.M., and Coon, M.J. (1996) Peroxo-iron and oxenoid-iron species as alternative oxygenating agents in cytochrome P450-catalyzed reactions: switching by threonine-302 to alanine mutagenesis of cytochrome P450 2B4. *Proc. Natl. Acad. Sci. USA* **93**, 4644-4648
40. Golly, I. and Hlavica, P. (1987) Regulative mechanisms in NADH- and NADPH-supported N-oxidation of 4-chloroaniline catalyzed by cytochrome b_5-enriched rabbit liver microsomal fractions. *Biochim. Biophys. Acta* **913**, 219-227
41. Hrycay, E.G., Gustafsson, J.A., Ingelman-Sundberg, M., and Ernster, L. (1976) The involvement of cytochrome P-450 in hepatic microsomal steroid hydroxylation reactions supported by sodium periodate, sodium chlorite, and organic hydroperoxides. *Eur. J. Biochem.* **61**, 43-52
42. Ruf, H.H. and Eichinger, V. (1982) Microsomal electron transport. The rate of the electron transfer to oxygenated cytochrome P450 in *Cytochrome P450, Biochemistry, Biophysics and Environmental Implications* (Hietanen, E., Laitinen, M., and Hänninen, O., eds.) pp. 597-600, Elsevier Biomedical Press, Amsterdam
43. Gillam, E.M.J., Baba, T., Kim, B.R., Ohmori, S., and Guengerich, F.P. (1993) Expression of modified human cytochrome P450 3A4 in *Escherichia coli* and purification and reconstitution of the enzyme. *Arch. Biochem. Biophys.* **305**, 123-131
44. Larson, J.R., Coon, M.J., and Porter, T.D. (1991) Purification and properties of a shortened form of cytochrome P450 2E1: deletion of the NH_2-terminal membrane-insertion signal peptide does not alter the catalytic activities. *Proc. Natl. Acad. Sci. USA* **88**, 9141-9145